Modeling sound scattering using a combination of the edge source integral equation and the boundary element method

Sara R. Martin,[1] U. Peter Svensson,[1] Jan Slechta,[1] and Julius O. Smith[2]

[1] *Acoustics Research Centre, Department of Electronic Systems, Norwegian University of Science and Technology, NO-7491 Trondheim, Norway*

[2] *Dept. of Music - Ctr. for Comput. Res. in Music and Acoust. (CCRMA), Stanford Univ., 660 Lomita Dr., Stanford, CA 94305*

(Dated: 11 June 2018)

A hybrid method for sound scattering calculations is presented in this paper. The boundary element method (BEM) is combined with a recently developed edge source integral equation (ESIE) [J. Acoust. Soc. Am. 133, pp. 3681-3691, 2013]. Although the ESIE provides accurate results for convex, rigid polyhedra, it has several numerical challenges, one of which applies to certain radiation directions. The proposed method, denoted ESIEBEM, overcomes this problem with certain radiation directions by applying a similar approach as BEM. First, the sound pressure is calculated on the surface of the scattering object using the ESIE, then second, the scattered sound is obtained at the receiver point using the Kirchhoff-Helmholtz boundary integral equation, as BEM does. The three methods have been compared for the scattering by a rigid cube. Based on results from several discretizations, ESIE and ESIEBEM results are typically (90% quartile) within $3 - 4 \cdot 10^{-4}$ for a kL-value of 1.83 and $2 \cdot 10^{-3}$ for $kL = 9.15$, L being the cube length, of reference results computed with the BEM. The computational cost of ESIEBEM appears to be lower than BEM.

I. INTRODUCTION

Accurate and fast numerical modelling of sound propagation and scattering is of great interest nowadays. A wide range of problems ranging from environmental acoustic problems to musical instrument synthesis require the modeling of large scale 3D computational domains. The computational complexity of standard solution methods such as the finite element method (FEM), boundary element method (BEM) and finite differences in the time domain (FDTD), scale poorly with the problem size. Therefore, alternatives to these well known methods are needed. The fast multipole boundary element method (FMBEM) is an alternative method to accelerate the calculations of the boundary element method[1] by clustering boundary elements and using multipole expansions to evaluate the interactions among clusters.

A recent edge source integral equation method (ESIE) presented by Asheim and Svensson[2] has shown to be more efficient computationally than the numerical methods mentioned above for convex, rigid scattering objects. Instead of using a mesh for the whole body surface (BEM), and possibly also the air surrounding the object (FEM, FDTD), only a discretization of the object edges is needed to compute so-called edge source amplitudes. In a subsequent stage, these edge source amplitudes can be used for computing the sound pressure in any external receiver positions, similar to the BEM, where the surface sound field can be used in a similar way. It has not been possible to prove that the ESIE method fulfills the governing Helmholtz equation, only that the results are remarkably accurate for rigid, convex scattering bodies. Although this method is very attractive computationally, and in terms of accuracy in general, erroneous results may arise for certain receiver positions[3].

The goal of this paper is to propose a method that achieves fast calculation while maintaining good accuracy. The method developed is a combination of the edge source integral equation (ESIE) method and the boundary element method (BEM). Parts of this work were presented in the POMA paper[4] by the same authors. The method avoids the singularities for certain receiver positions of the ESIE[3], and it also avoids the well-known internal resonance phenomenon of the BEM formulation commonly avoided by using the Burton and Miller's method[5] or the CHIEF points technique[6]. The computational cost of this hybrid method will be compared to the BEM and to the original ESIE.

This paper is organized as follows: in section II, the fundamental equations and theoretical backgrounds for the three methods, the boundary element method (BEM), the edge diffraction-based ESIE method and the hybrid method are introduced. Section III summarizes the implementation details of the methods as well as the description of the benchmark case, and the results obtained are presented and discussed in section IV. Finally, section V collects the conclusions of the paper.

II. THEORY

There are two large families of methods for solving acoustic scattering problems: those commonly called wave-based techniques derived from the wave equation (BEM, FDTD, FEM, FMBEM) and those referred to as geometrical-acoustics techniques which are high frequency assymptotic solutions (the image source method, ray tracing). The latter can also have diffraction-based extensions such as the geometrical theory of diffraction (GTD) presented by Keller[7], the Uniform Theory of Diffraction (UTD) by Kouyoumjian and Pathak[8], or the recent edge source integral equation method (ESIE) by Asheim and Svensson[2] mentioned above. Two of these methods will be presented more in detail below: the wave-based boundary element method, and the edge source integral equation method. Their respective advantages and drawbacks will be identified, and a new hybrid method will be presented that exploits the advantages of both techniques and avoids some of their limitations when combined to solve scattering problems.

A. The boundary element method (BEM)

The acoustic boundary element method is a well-established method in acoustics, especially suitable for infinite domains (outdoor/free-field environment). The BEM formulation is based on the Helmholtz integral equation which relates the sound pressure $p(P)$ at any point P to the sound pressure $p(Q)$ and the normal velocity $v_n(Q)$ at positions Q on the surface D of a scattering body. In this paper, only rigid scattering polyhedra will be studied and so the Neumann condition $v_n(Q) = 0$ holds for any point $Q \in D$. Therefore, the Helmholtz integral equation for these cases can be expressed without the monopole term and it can be written as follows[9]

$$C(P)p(P) = 4\pi p^I(P) + \int_D \frac{\partial G(P,Q)}{\partial \mathbf{n}} p(Q) dS, \tag{1}$$

where $G(P,Q) = \dfrac{\mathrm{e}^{-\mathrm{j}kR}}{R}$ is the free-field Green's function in 3D between two points P and Q, R is the Euclidean distance between P and Q, p^I is the incident sound pressure, $C(P)$

is the solid angle corresponding to 0, 2π or 4π if P is inside, on the surface, or outside of the object, respectively, k is the wavenumber, and $\mathbf{n}$ is the normal vector to the surface at Q pointing away from the body. A time-harmonic factor $\mathrm{e}^{\mathrm{j}\omega t}$ has been omitted in Eq. (1) and throughout the paper.

The sound pressure at any point P expressed in Eq. (1) is interpreted here as a sum of contributions from free-field radiating dipoles aligned with the surface normal vector. The strength of the dipole is given by the surface sound pressure and once this sound pressure on the surface is known, then the sound pressure at any point P can be obtained.

The boundary element method calculates the sound pressure in a field point P in two steps. In the first step, the solution on the surface of the scattering object is obtained by placing P on the surface of the scattering object, and Eq. (1) becomes an integral equation. In the second step, the so-called ”propagation” step, the sound pressure in the sound field is calculated by letting P be an external point, often termed as a ”field point”.

Different discretization methods are commonly used for the first step, such as the projection methods (Galerkin, collocation) or Nyström methods, which turn Eq. (1) into various forms of linear systems of equations. The number of degrees of freedom in that system of equations is directly related to both the accuracy of the solution and the computational cost.

The BEM, when it is applied to exterior scattering problems, has a well-known problem as mentioned in the introduction. The matrix equation to solve becomes ill-conditioned at the natural frequencies of the corresponding interior problem, but two different solutions have been presented in the literature for this problem. A first technique is using so-called

CHIEF points, or internal control points, where the sound field is enforced to be zero[6]. A second one is the so-called Burton-Miller technique[5] which uses a linear combination of the Kirchhoff-Helmholtz integral equation and its normal derivative. Marburg and Amini[10] show that the Burton and Miller method is a more robust method compared to the CHIEF method as its solution is unique for exterior acoustic problems at all frequencies[10].

Another challenge of the BEM is the singularity in the integral kernels, which becomes prominent for thin bodies and narrow gaps[11] as well as when the field point is located near the boundary of the scattering object. There have been different approaches to overcome that difficulty making use, for instance, of singular numerical integration as suggested by Cutanda et al.[12], splitting the integral using analytical removal of the singularity[11,13], or using a polar coordinates transformation as presented by T. Terai[14]. The details of these techniques will not be discussed in this paper and the interested reader is referred to the cited work for more details.

B. Edge source integral equation method (ESIE)

The edge-diffraction based method used in this paper is the edge source integral equation (ESIE) method suggested recently by Asheim and Svensson[2]. This method, which was shown to be accurate and efficient for rigid convex scattering objects, decomposes the total acoustic field into three different components:

$$p_{tot}(P) = p_{GA}(P) + p_{D1}(P) + p_{HOD}(P), \tag{2}$$

where $p_{GA}(P)$ is the geometrical acoustics component, and $p_{D1}(P)$ and $p_{HOD}(P)$ correspond to the first- and higher-order diffraction components respectively. The geometrical acoustics term, p_{GA}, represents the direct and reflected sound considering the visibility between source and receiver, and it can easily be obtained by the commonly used image source (IS) method.

The first-order diffraction is based on a representation of the diffracted field for a single wedge[15], which is a reformulation of the analytical solution for infinite edges by Bowman and Senior[16] that can be applied to finite edges.

This first-order diffraction term in Eq. (2) at a receiver's position P, $p_{D1}(P)$, can thus be computed as an explicit line-integral equation over the set of edges Γ of the scattering object as

$$\begin{aligned} p_{D1}(P) = &-\frac{1}{4\pi} q_S \nu_z \\ &\times \int_{\Gamma} V_{P,z} V_{z,S} \frac{\mathrm{e}^{-\mathrm{j}kr_{P,z}}}{r_{P,z}} \frac{\mathrm{e}^{-\mathrm{j}kr_{z,S}}}{r_{z,S}} \beta(P,z,S) dz, \end{aligned} \quad (3)$$

where q_S is the source strength of the sound source, S, defined such that $q_S = \rho_0 A/4\pi$, where ρ_0 is the density of the medium at rest, and A is the volume velocity amplitude of the monopole sound source. In Eq. (3) ν_z is the so-called wedge index, $V_{a,b}$ is a point-to-point visibility term being one when a is visible from b and zero otherwise. The term $\beta(P, z, S)$ is a function which depends only on the wedge angle and on the angles of the sound source, S, and receiver, P, defined relative to the tangent at the edge point z, and thus β is interpreted as a directivity function of a virtual/secondary edge source at point z[15]. The integral in

Eq. (3) can be computed by standard quadrature methods or, as suggested by Asheim and Svensson, by employing the efficient and accurate numerical method of steepest descent[17].

The higher-order diffraction term, p_{HOD}, is obtained by the introduction of explicit edge source strengths for the secondary sources along the edges referred to above, for first-order diffraction. The computation process is similar to the BEM in that first, the strengths of these secondary edge sources are calculated by solving an integral equation and secondly, the diffracted sound pressure, p_{HOD}, is obtained via a propagation integral from the edge sources to the receiver. Below is a brief description of the formulation to obtain p_{HOD}.

Let $q(z_1, z_2)$ be defined as the equivalent source strength at an edge point z_2 radiating in the direction of another edge point z_1. As shown by Asheim and Svensson[2], $q(z_1, z_2)$ needs to satisfy the following integral equation

$$q(z_1, z_2) = q_0(z_1, z_2) - \frac{1}{8\pi} \int_\Gamma q(z_2, z) \cdot \frac{\mathrm{e}^{-\mathrm{j}kr_{z_2,z}}}{r_{z_2,z}} \times \nu_{z_2} V_{z_1,z_2} V_{z_2,z} \beta(z_1, z_2, z) \mathrm{d}s_z. \quad (4)$$

The term $q_0(z_1, z_2)$ corresponds to the equivalent source strength at z_2 due to the field diffracted at z_2, coming from the source S, in the direction of z_1 which is expressed as follows

$$q_0(z_1, z_2) = -\frac{1}{8\pi} \nu_2 V_{z_1,z_2} V_{z_2,S} \frac{\mathrm{e}^{-\mathrm{j}kr_{z_2,S}}}{r_{z_2,S}} \beta(z_1, z_2, S). \quad (5)$$

Once the edge source strengths are obtained, by solving the integral equation (4), the term $p_{HOD}(P)$ can be computed by a double integral, each integration taken along the set of all edges, expressed as follows

$$p_{HOD}(P) = -\frac{1}{8\pi}\int_\Gamma\int_\Gamma q(z_1,z_2)\nu_{z_1}V_{P,z_1}V_{z_1,z_2} \times \frac{\mathrm{e}^{-\mathrm{j}kr_{P,z_1}}}{r_{P,z_1}}\frac{\mathrm{e}^{-\mathrm{j}kr_{z_1,z_2}}}{r_{z_1,z_2}}\beta(P,z_1,z_2)\mathrm{d}s_{z_2}\mathrm{d}s_{z_1}, \quad (6)$$

where the spherical radiation factors and the same directivity function β as used in Eq.(3) have been considered.

Note that the computation of the edge source strengths $q(z_1, z_2)$ in Eq.(4) is independent of the receiver's position in the same way as the first step of the BEM when computing the sound field at the surface of the scattering object. The attractiveness of the ESIE, though, is that there is only the need to discretize the edges of the object instead of the entire surface, which reduces considerably the computational cost. A further advantage of the ESIE versus the BEM is that the ESIE does not have any problem with the internal fictive resonances that the BEM suffers from. On the other hand, the intermediate quantities are more directly useful for the BEM than for the ESIE: the surface sound pressure might be exactly what is sought in some applications, whereas those edge source amplitudes are apparently not useful for anything by themselves.

The ESIE gives very accurate results for rigid convex scattering objects (so, with no indents) and even gives accurate results in the low-frequency limit[2]. As mentioned in the Introduction, it has not been shown that the ESIE method should give an exact solution to the Helmholtz equation. Very accurate results have been demonstrated nevertheless, and it is not clear how this conundrum can be tackled. But, for certain receiver positions, the convergence to the accurate solution for the propagation step is very slow due to that the directivity function β in Eq.(6) has some singularities that depend on the positions of the receiver P relative to the edge sources z_1 and z_2. Two edges define a virtual plane, exterior to the scatterer, and the directivity function β makes a jump as a receiver position crosses that virtual plane[3]. Associated with that jump is a very slow convergence.

Since the β-function is also used in the expression for the term q_0, in Eq. (5), there will be inaccurate results associated with external source positions that are very near to any of the planes that are formed by pairs of the scattering body's edges. Finally, the presence of the β-function in the integral equation operator in Eq. (4) leads to slow convergence when smooth scattering objects are represented by polyhedra. Interestingly, the ESIE formulation is numerically much more efficient for scattering bodies with edges than for smooth bodies.

C. Combining the ESIE and the BEM: ESIEBEM

It is possible to combine the two presented methods in a way that uses their respective strengths and overcomes some of their respective weaknesses. The hybrid method proposed here, called the ESIEBEM from now on, is based on using the ESIE, instead of the Helmholtz integral equation, for obtaining the sound pressure on the surface. At this calculation stage, the surface of the object is discretized by an element mesh and the sound pressure is computed at the element centers (collocation points). The expression of the directivity function β for this case, appearing in both Eq. (3) and Eq. (6), has been derived in the Appendix VII. Note that β would have no singularity related to the receivers positions on the surface, except for source positions close to a plane of the scattering object (as discussed in Section II B). There is also a $1/r$-singularity, where r is the distance from the receiver point to and edge point, which is the reason to use collocation points instead of the element nodes. However, the computation of the directivity function β will still have some challenges when two or more faces of the scattering polyhedron are close to co-planar.

The principles of the ESIE and ESIEBEM are illustrated in Fig. 1. The ESIEBEM involves three calculation steps. The first step is the same as for the ESIE: calculation of the edge source strengths, given the external source, using Eqs. (4) and (5). The second step is the edge source-based computation of the sound pressure in the element collocation points on the surface, using Eq. (2), (3), and (6) and the third step employs the propagation integral of the BEM, Eq. (1).

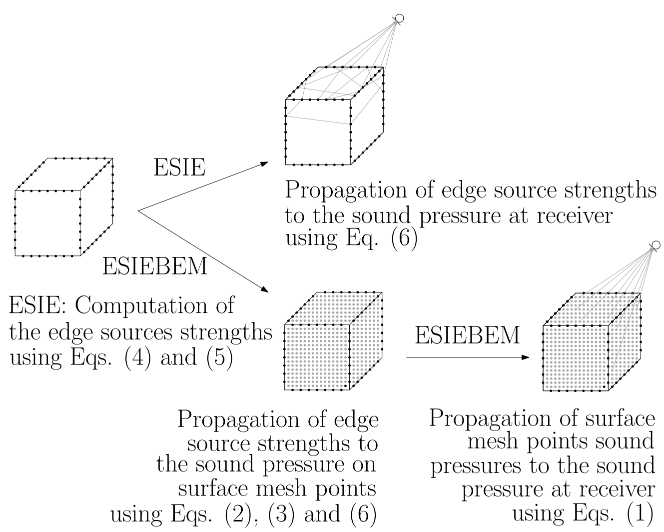

FIG. 1. Illustration of the ESIE and the ESIEBEM computation steps. The discretization of edges and surfaces as well as paths drawn are only a few, for illustration purposes.

The main advantage of using the ESIE in this first step of computing the sound pressure on the surface is that the ESIE is highly efficient for finding the sound pressure in receiver positions that are not challenging for the method. Therefore, the computation time might be advantageous compared to the BEM. Moreover, the accuracy of the ESIEBEM seems to be guaranteed as long as the receiver points on the surface are not immediately at the edge[3] and the scatter has no co-planar faces.

III. IMPLEMENTATION

A. BEM - Direct collocation method

In this paper, the OpenBEM implementation developed by Juhl and Henriquez has been used for obtaining the BEM results. OpenBEM is a collection of open-source Matlab functions for solving acoustical problems in 2D, 3D or axi-symmetric settings[18]. Interested readers will find a detailed description of it in Ref.[19] by Juhl and a shorter version of it in Ref.[20] by Henriquez and Juhl.

The implementation employs the direct collocation method to compute the sound pressure on the scattering body surface. The scatterer's surface is discretized into a mesh of elements, triangular or quadrilateral, and the sound pressure is calculated at the nodes of this mesh. When the point P in Eq. (1) is placed at any node, the following matrix expression results

$$\mathbf{Cp} = \mathbf{Ap} + 4\pi \mathbf{p}^{\mathbf{I}}, \tag{7}$$

where the matrix $\mathbf{A}$ contains integrals of the kernel functions defined in Eq. (1).

Since rigid scattering objects are considered in this paper, the Neumann boundary condition applies, i.e., $v_n(Q) = 0$, and the left-hand side term in the expression can be directly substracted from the diagonal of the first term on the right-hand side, and Eq. (7) is simplified to

$$\mathbf{p} = \mathbf{D^{-1}}(-4\pi\mathbf{p^I}), \tag{8}$$

where $\mathbf{D} = \mathbf{A} - \mathbf{C}$ is a full matrix. If the surface mesh used has N elements, then the computational complexity to solve the scattering problem with the OpenBEM is of the order of N^2, for building up the needed matrices, with a subsequent step scaling as N^3 for inverting the matrix. The simple Gauss elimination is used here to solve Eq. (8), although other more efficient iterative solvers could have been implemented, and reduced the complexity by an order of magnitude. The minimum number of surface elements will depend on the square of the maximum frequency studied, f_{max}, so the total computation time might scale as $T_{\mathrm{comp}} \sim f_{\mathrm{max}}^4 - f_{\mathrm{max}}^6$, depending on which stage is computationally dominating in a specific implementation.

The OpenBEM uses the common method with CHIEF points to avoid the problems at certain fictive internal resonance frequencies[6].

B. ESIE - Matrix equation formulation

The ESIE method used in this paper was implemented in Matlab by Svensson et al.[21] as the "Edge diffraction toolbox" published under the terms of the GNU General Public License and currently available on GitHub. The toolbox computes various combinations of specular reflections and higher-order diffraction, in the frequency domain.

The ESIE is based on the solution of the integral equation in Eq. (4) where the unknown edge source strengths $q(z_1, z_2)$ need to be solved for each pair of edge points (z_1, z_2). This is done using the straightforward Nyström, or quadrature, method, where the integral equation is discretized at positions z^i along all the straight edges of the polyhedron. The unknowns are the edge source strengths, defined for pairs of discrete points along the edge, $q(z_1^i, z_2^j)$, which refer to the edge source amplitude at edge point z_2^j, in the direction of edge point z_1^i. For each straight edge of the polyhedron, a Gauss-Legendre (G–L) quadrature scheme is employed. A certain G–L quadrature order is chosen for the longest edge, and proportionally lower orders are chosen for shorter edges. For a cube example, if each of the 12 edges are discretised according to a G–L quadrature order n_{gauss}, a total of $12 \cdot n_{gauss}$ edge points will consequently be generated. As discussed further below, each edge point of a cube can reach 6 other edges, and thus $6 \cdot n_{gauss}$ other edge points, for a total of $72 \cdot n_{gauss}^2$ unknowns. By constructing a column-vector $\mathbf{q}$ with all the terms $q(z_1^i, z_2^j)$, z_1^i and z_2^j being the discretization points of all edges, Eq. (4) can be rewritten as the matrix expression

$$\mathbf{q} = \mathbf{q_0} + \mathbf{Hq}, \tag{9}$$

where the matrix $\mathbf{H}$ contains sampled values of the kernel of the integrand operator in Eq. (4), including the weighting factors of the Gauss-Legendre quadrature rule. This matrix equation can be solved by inversion

$$\mathbf{q} = [\mathbf{I} - \mathbf{H}]^{-\mathbf{1}}\mathbf{q_0}, \tag{10}$$

although the size of the $\mathbf{H}$-matrix often prohibits such a direct inversion. Fortunately, $\mathbf{H}$ has a very sparse nature, which makes an iterative solution of Eq. (9) very efficient[2]. Thus, iteration step n gives a term

$$\mathbf{q}_n = \mathbf{H}\mathbf{q}_{n-1}, \qquad n \in \mathbb{N}, \tag{11}$$

where $\mathbf{q}_0$ is given by sampled values of Eq. (5), and all terms of the truncated iteration process are summed up to the final solution,

$$\mathbf{q}_{\text{final}} = \sum_{n=0}^{N_{\text{truncation}}} \mathbf{q}_n, \tag{12}$$

The final solution is then propagated to the receiver with Eq. (6), and the term p_{HOD} obtained will correspond exactly to the contribution of all orders of diffraction up to and including order $(N_{\text{truncation}} + 2)$. The matrix equation formulation for this propagation is

$$p = \mathbf{F}\mathbf{q}_{\text{final}}, \tag{13}$$

where p is the sound pressure amplitude in a single receiver point, and $\mathbf{F}$ is a horizontal vector of samples of the integrand in Eq. (6), again with weighting factors according to the Gauss-Legendre quadrature.

The sparseness of the matrix $\mathbf{H}$ is the reason for the efficiency of the ESIE, and it is explained in Appendix VIII. The minimum number of edge points/sources, N_{es} will scale as $N_{\text{es}} \sim f_{\text{max}}$, whereas the number of edge source amplitudes, N_q will scale as $N_{\text{q}} \sim N_{\text{es}}^2 \sim f_{\text{max}}^2$. The size of the $\mathbf{H}$-matrix is such that the number of non-zero terms is $\sim N_{\text{q}}^{3/2}$, so the iterative solution of the matrix equation will cost $T_{comp} \sim f_{\text{max}}^3$. This suggests that the ESIE could indeed be more efficient than the BEM for computing the field at the surface of the scattering body.

C. ESIEBEM

The hybrid method ESIEBEM suggested in this paper employs the discretization of the scatterer's surface like the BEM does. Triangular elements are used in this paper rather than quadrilateral elements but the hybrid method might be used with quadrilateral meshing as well.

As mentioned earlier in the text, it is known that the ESIE converges very slowly for receiver positions where the visibility factor suddenly changes from 0 to 1, along the zone boundaries that extend away from the scattering polyhedron. Receiver positions on the surface of the scattering bodies are, however, not exposed to this problem. On the other hand, along the edges of the scattering polyhedron, there are numerical challenges for the ESIE, caused by the $1/r$-factor in the involved integrals. No scheme has been developed for mitigating this singularity, and therefore the standard quadrature method that is employed here becomes inefficient for receiver positions very close to the edge. However, if the surface sound pressure is calculated at element center points (i.e. collocation points) rather than at the nodes, the effect of this singularity is reduced. Improved schemes might be developed that handle that singularity more efficiently.

Yet another singularity occurs at the corners where two or more edges meet. The Gauss-Legendre quadrature approach does not use any quadrature points at the integration range endpoints, that is, at those corners, and no problems have been encountered with the quadrature used for the integral equation. A well-behaved polynomial convergence is demonstrated in section IV B, as long as receiver points are not close to any zone boundaries. Also, in Ref.[2], the case of a circular disc was studied in detail. For a symmetrical incident field, the integral equation could be simplified to a one-dimensional one, which was evaluated with the midpoint method, in order to avoid the same singularities at the endpoints of the integration range. No problems with convergence were encountered there either.

The internal-resonance problem and the thin-scattering-body problem mentioned in section II A that BEM encounters, do not apply to the ESIEBEM, but the near-singularity issue for field points near the scattering bodies applies for both, BEM and ESIEBEM. OpenBEM uses a refined quadrature scheme and the solution for the near-singular kernels could be either to increase the mesh density near the close point or to increase the order of the numerical integration[?] .

The test cases are calculated with different meshes when solving the problem with the BEM and ESIEBEM, and with different numbers of edge discretization points when solving the problem with the ESIE. The meshes have been created with the open-source GMSH software[22]. All elements are considered to be triangular and the receiver points (i.e. the collocation points of the elements) correspond to the center points of these triangular elements in the first ESIEBEM calculation step. The ESIEBEM uses isoparametric elements with constant shape functions and derivatives of these shape functions equal to zero, as employed in the OpenBEM.

D. Test case

The scattering object studied here is one of the simplest to test the performance of the novel hybrid method: a rigid cube as shown in Fig. 2. A cube of size 1 x 1 x 1 m^3 has been modeled centered at the origin, assuming an incident field of a sound source located very far away at a position $(x, y, z) = 10^6/\sqrt{3}(1, 1, 1)$ m, to emulate a plane wave impinging on the scattering object. The results shown in this section are for the frequencies 100 and 500 Hz, corresponding to $kL = 1.83$ and 9.15, respectively, where L is the side length of the cube.

The receiver positions are in the plane $z = 0$ along a 1 m radius circumference with a total of 629 receivers uniformly distributed, with a step of 0.01 radians, starting from 0. Twelve different meshes were constructed for the BEM, with 408, 624, 744, 1096, 1480, 3124, 6260, 10204, 13084, 20456, 30940 and 50872 elements. With the ESIE method, edges were discretized with 16, 24, 32, 40, 48, 56, 64, 80, and 96 edge points per edge, giving 192-1152 total edge points.

The calculations were carried out on a Macintosh HD with a processor of 2.7 GHz (Intel Core i5) and 16 GB RAM and on a desktop computer with an operating system Windows 10 and a processor Intel(R) Xeon(R) 3.4 GHz and 8.0 GB RAM.

IV. RESULTS

In this section, results will first be presented with the finest BEM-mesh results viewed as reference results. In the subsections following after, the application of linear extrapolation will be explored to reach a higher accuracy for all the methods.

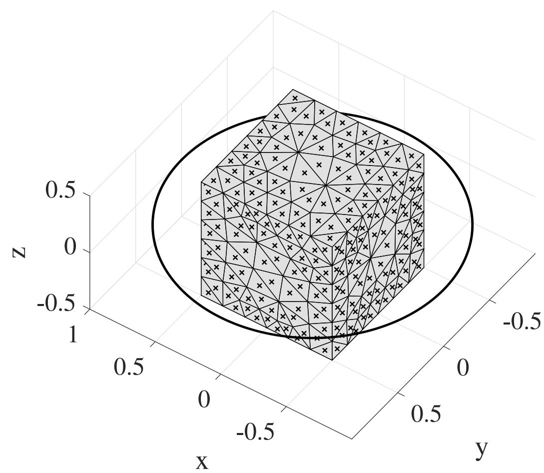

FIG. 2. Benchmark test case, a cube of 1x1x1 m^3 and 629 receivers located along a circumference of 1 m radius. Collocation points on the cube surface are depicted with black crosses. The same mesh with triangular elements is used both for the BEM and ESIEBEM, and the figure shows a coarse mesh for visualization purposes with 200 nodes and 396 collocation points.

A. Overcoming problematic positions for the ESIE by using the ESIEBEM

As explained in Section II B, the ESIE method has singularities for some receiver positions. To demonstrate this effect, the sound pressure has been computed for the two frequencies, 100 Hz and 500 Hz, and all 629 receivers indicated in Fig. 2 using a BEM mesh with 50872 elements and collocation points, and an ESIE discretization with 96 edge sources per edge, that is, $96 \cdot 12 = 1152$ edge sources and $96 \cdot 12 \cdot 96 \cdot 6 = 663552$ unknowns in the $\mathbf{q}$-vector (eq. 9). ESIEBEM then used the same numbers of surface mesh elements and edge sources.

Fig. 3 shows the sound pressure level difference for the methods ESIEBEM and ESIE, relative to the reference results given by the BEM for 100 Hz and for 500 Hz. It can be quite clearly seen that the ESIE has problems for some of the eight expected receiver angles, namely those that are very close to one of the infinite planes that contain the cube surfaces as mentioned in Section II B. Confirming one of the goals of developing the hybrid method, the ESIEBEM seems to give accurate results for those positions and therefore overcomes the singularities of the problematic receiver positions of the ESIE.

Comparing Fig. IV A and Fig. IV A, it can be observed that the sound pressure level difference between the two methods, ESIE and ESIEBEM, and the reference result given by BEM, is in much better agreement for 100 Hz than for 500 Hz. The mesh sizes are the same for both calculations so the number of elements per wavelength is five times higher in case (a) than in case (b).

Two receivers have been chosen and depicted in Fig. 3 for further study in the next sections: R_1 at 142.6° is a non-problematic receiver for ESIE and R_2 at 239.5° is a receiver close to a singularity of the ESIE propagation integral in Eq. 6.

B. Convergence for the three methods

Each method has been run for different discretizations and here, the convergence of each method towards their respective final value is analyzed further.

The potential for using extrapolation to find an estimate of the ultimate/final result, for an infinitely large number of elements, is explored below. This is the same technique as is used in Richardson extrapolation, where it is assumed that each computed value, p_n, based on a discretization step, Δh_n, is governed by a Taylor expansion around the final value,

$$p_n = p_{\text{final}} + C_0 \Delta h_n^{k_0} + ... \tag{14}$$

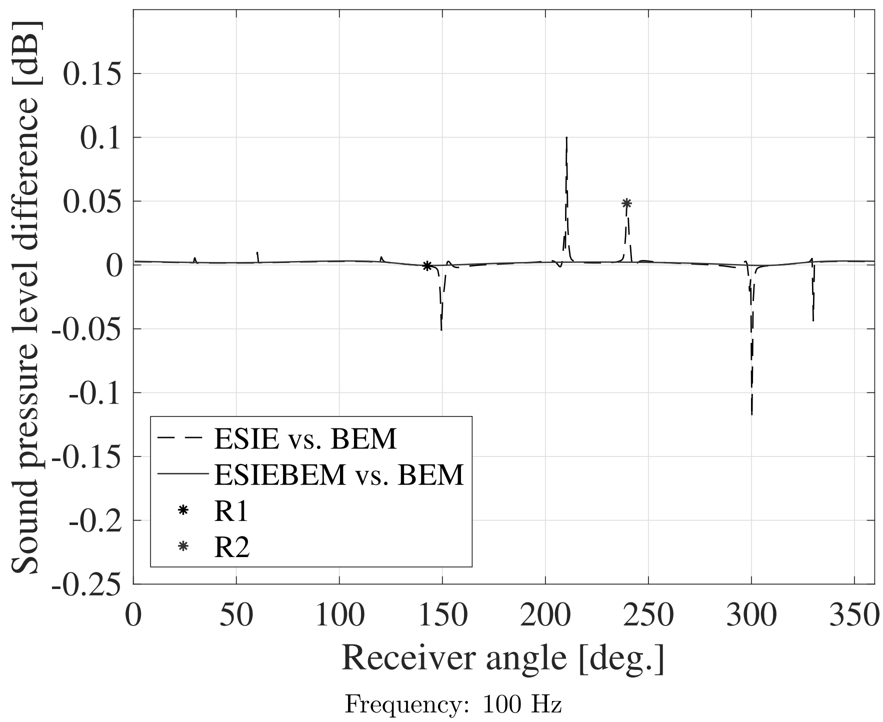

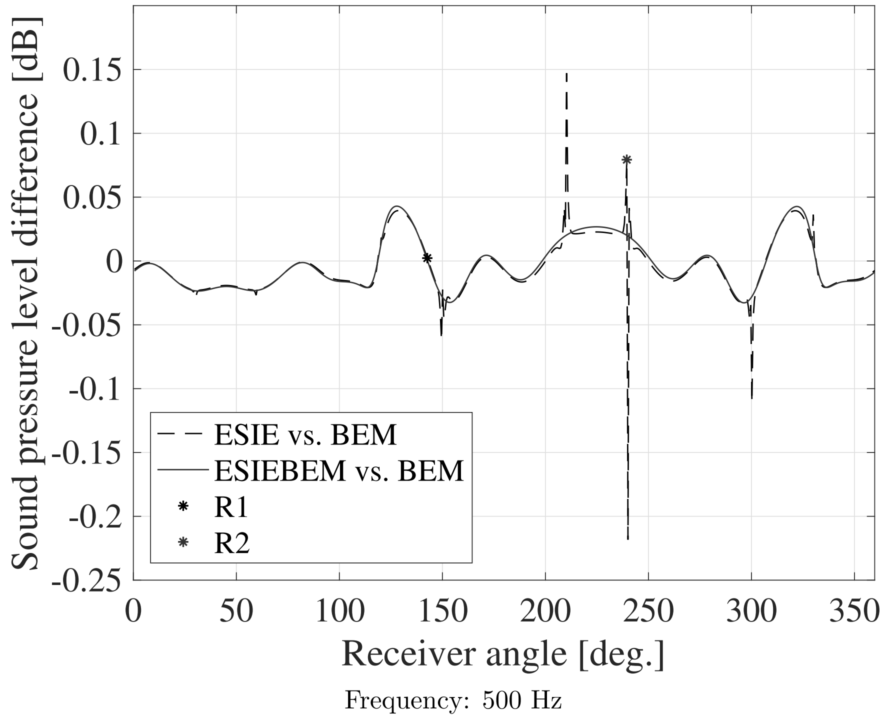

FIG. 3. Sound pressure level difference as function of the receiver angle for the 629 receivers in Fig. 2. Reference method is the BEM with 50872 elements. Two receiver positions are marked, R_1 and R_2, that will be studied further. The frequency is: a) 100 Hz and b) 500 Hz.

where k_0 is a known or unknown exponent of the error convergence for the method at hand, and only the first polynomial term is kept. For the methods employed here, the sought value p_{final} can be found via a straight line fit to the data points p_n against 1/BEM-mesh-size, for the BEM and ESIEBEM results and 1/ESIE-edgesource-number^2 for the ESIE results. The final value would then be the intersection of the straight line with the y-axis representing a potential value for an infinite mesh of each method respectively.

Fig. 4 shows one example for the real part of the sound pressure amplitude at 100 Hz for all three methods, for receiver R_1 at 142.6° chosen in the previous section. The results are plotted versus 1/BEM-mesh-size for the BEM and ESIEBEM, and 1/ESIE-edgesource-number^2 multiplied by 10^2 for visual purposes, respectively. The four finest discretizations for each method have been used for a straight line-fit, and the subsequent extrapolation to the y-axis crossing will be an estimate of the p_{final} values for each method.

It can be seen that the results for all three methods follow a trend that becomes rather linear for the finer discretizations, which supports the expected error convergence exponent: BEM and ESIEBEM converge as $\mathcal{O}(1/N)$ and ESIE as $\mathcal{O}(1/N^2)$. As a sidenote, it can be pointed out that a uniform discretization of the edges in the ESIE gives a $\mathcal{O}(1/N)$-convergence, so the Gauss-Legendre quadrature used in the implementation gives a much better accuracy for practically the same computational cost.

An interesting way to evaluate the convergence of these results is presented here. Figs. 5 and 6 show the trajectories of the complex sound pressure amplitude, as the discretization is refined, for all three methods, for the two different receivers R_1 and R_2, for 100 Hz (Fig.

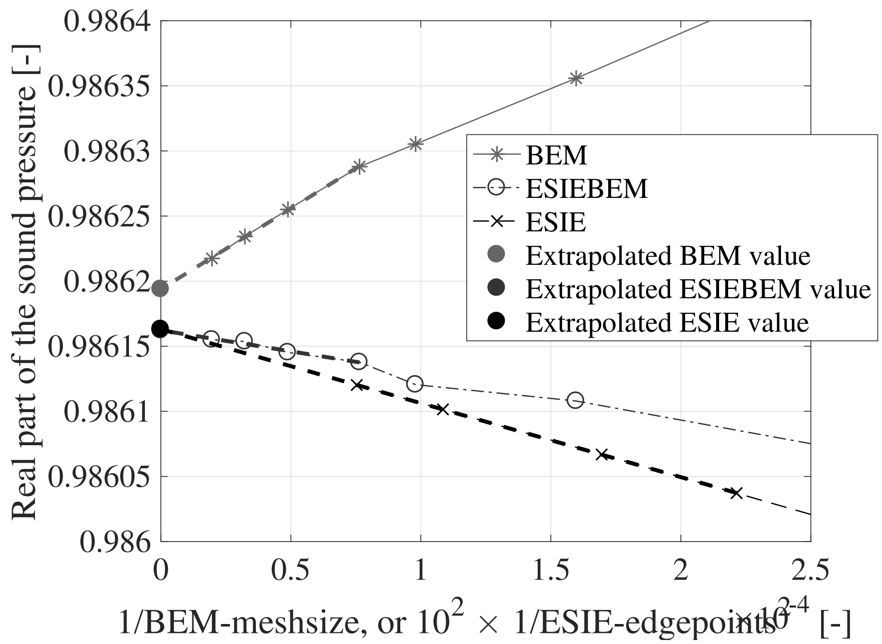

Receiver R_1

FIG. 4. Real part of the sound pressure amplitude at 100 Hz and receiver R_1, computed with a number of different discretizations for the BEM, ESIEBEM, and ESIE method. The results for the four finest discretizations have been used for the linear regression.

5) and 500 Hz (Fig. 6), respectively. Also the extrapolated values obtained for each method have been plotted, except for the ESIE method at R_2 since this receiver is near a singularity location and its extrapolated value can not be determined.

It can be seen that for receiver R_1 the ESIE and ESIEBEM converge to its final value quite quickly and with a smooth and uniform trajectory, while the BEM takes larger steps.

For the ESIE problematic receiver, R_2, it can be observed that the final value is not at the end of a smooth trajectory, since the results jump back and forth as the discretisation is increased. The singularity of the ESIE for those problematic positions might be solved by simply refining enough the discretization of the integration points. However, the convergence

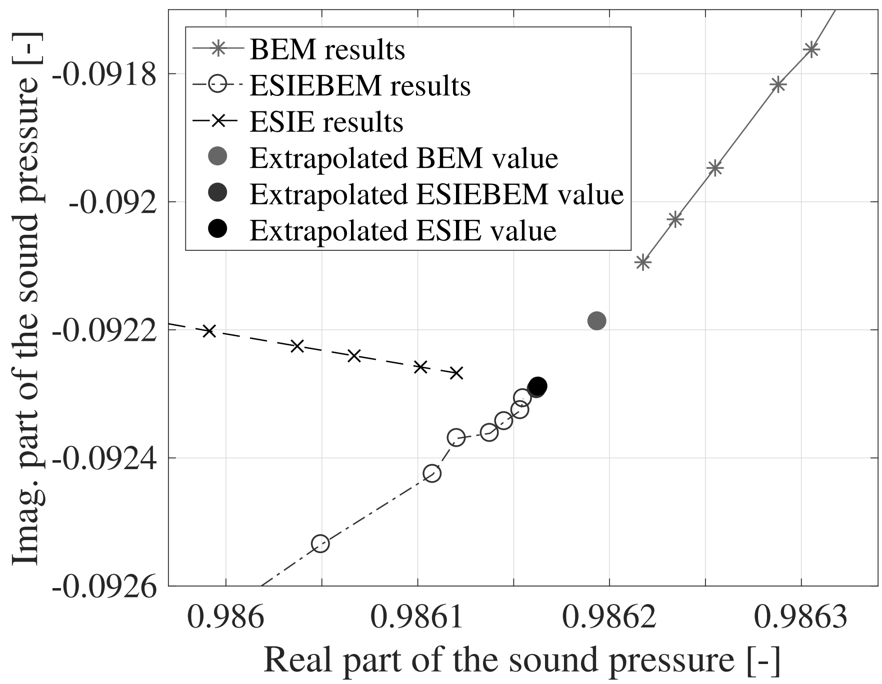

Receiver R_1

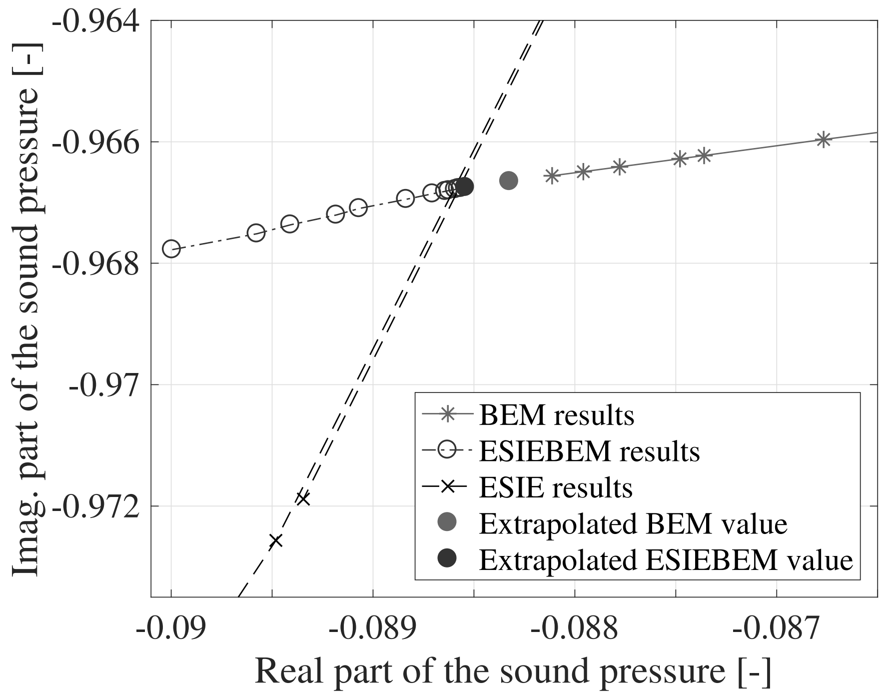

Receiver R_2

FIG. 5. Convergence for the BEM, ESIE and ESIEBEM for the cube test case at 100 Hz. The sound pressure amplitude is plotted in the complex plane and each point corresponds to a different mesh size or to a different number of edge sources, for a) receiver R_1, and b) receiver R_2

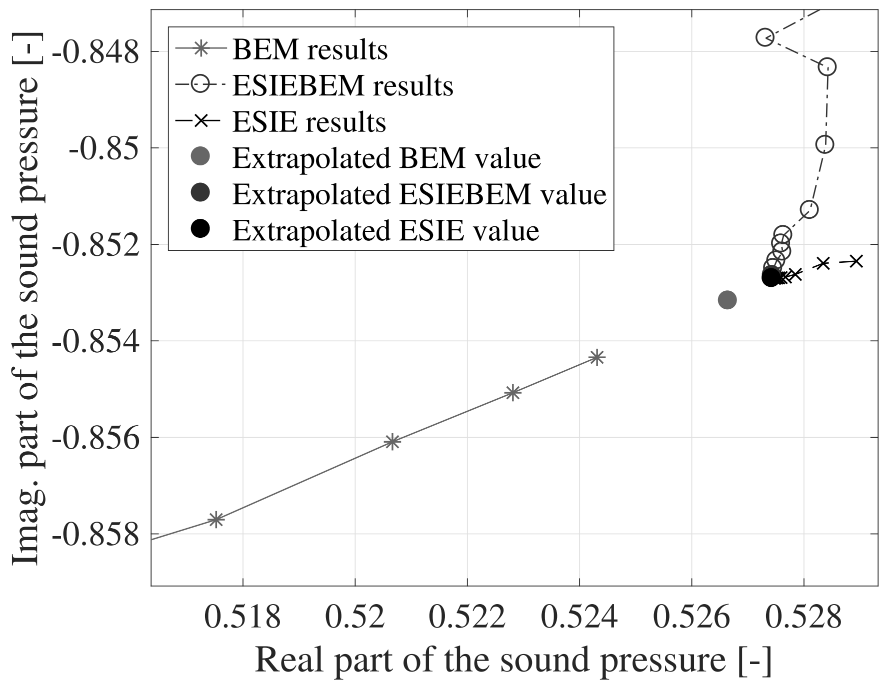

Receiver R_1

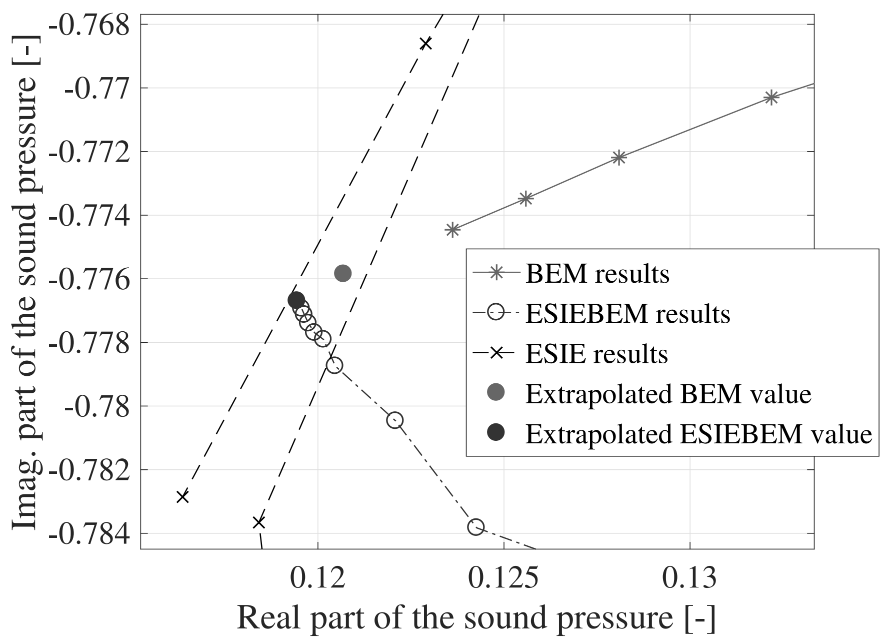

Receiver R_2

FIG. 6. Convergence for the BEM, ESIE and ESIEBEM for the cube test case at 500 Hz. The sound pressure is plotted in the complex plane and each point corresponds to a different mesh size or to a different number of edge sources, for a) receiver R_1, and b) receiver R_2

is very slow and it is not clear that the refining would ultimately converge to the correct result.

It is also interesting to notice that the extrapolated estimates of the result with the finest meshes for each method are much closer to each other than the results for the finest discretizations themselves. Certainly, the value of p_{final} that is found in the way explained above (see Eq. (14)) is not the ultimate result, but it can be viewed as a more accurate estimate of the ultimate result than the best computed result, $p_{n,max}$ with the finest discretization.

Now, the convergence of each method towards their respective final value, p_{final}, can be studied. For each receiver, the relative error is computed with this extrapolated estimate of the final result used as reference result,

$$\epsilon^i_{\text{rel}} = \left| \frac{\hat{p}_i - p_{\text{ref}}}{p_{\text{ref}}} \right|, \tag{15}$$

where $\hat{p}_i$ is the sound pressure at receiver i and p_{ref} the reference sound pressure, in this case, $p_{\text{ref}} = p_{\text{final}}$. This relative error will vary among receiver positions, with potentially very large variations, so here the median value, rather than the mean, across receiver positions is presented as follows. Figs. IV B and IV B present the median relative error over all the receivers as function of BEM-mesh elements and number of edge sources, for the frequencies 100 Hz and 500 Hz, respectively. The median has been chosen here rather than the mean or the maximum absolute error to basically remove the well known inaccurate results given by ESIE for certain receiver positions as discussed earlier.

All three methods display convergences with the assumed rates. Notably, the use of the extrapolated result as a reference, rather than the result for the finest discretization, makes these curves follow the trends very well. It is worth to mention that those rates would increase in case polynomials of higher order in BEM or ESIEBEM were used. Apparently, the ESIE converges to the extrapolated value with the fastest rate and the ESIEBEM converges to its extrapolated value with smaller error than the BEM. Thus, the hybrid ESIEBEM method developed in this paper, is performing very well compared to the boundary element method. It is interesting to note that the ESIE results reach similar accuracies for both frequencies, 100 Hz and 500 Hz. The error of BEM and ESIEBEM, on the other hand, gets one order of magnitude higher from the results at 100 Hz to the ones at 500 Hz, which is not surprising since the discretizations are the same for both frequencies.

It should also be realized that the reference result in Fig. 7 was computed from the results of each method to demonstrate the method's convergence. The studied acoustic scattering problem does not have an analytical solution, but the extrapolation of the BEM can be considered as a reference result to compare the results of the methods. Fig. 8 shows different measures of the relative error (over all receivers) using the BEM extrapolation value as a reference p_{ref} in Eq. 15, in this case, $p_{\text{ref}} = p_{\text{final,BEM}}$, for 100 Hz (Fig. IV B) and 500 Hz (Fig. IV B): the maximum error, the 90% percentile, the mean error and the 50% percentile (the median) over all 629 receivers for each of the three methods. First, it is interesting to notice the significant difference between the maximum error and the 90% percentile for the ESIE which is due to the well known problematic receivers. This effect causes the mean and the median errors for the ESIE to be quite different too, and as mentioned earlier, that is the reason to make use of the median rather than the mean in Fig. 7. For ESIEBEM and BEM, both the maximum error and the 90% percentile are quite close, as well as the median and the mean errors.

It can also be observed that the ESIE and ESIEBEM have smaller errors relative to the BEM extrapolation than the proper BEM up to a certain fine BEM mesh. The relative errors of the ESIE and ESIEBEM typically (90% quartile) reach $4 \cdot 10^{-4}$(ESIE) and $3 \cdot 10^{-4}$ (ESIEBEM) at 100 Hz, and $2 \cdot 10^{-3}$ at 500 Hz, relative to the extrapolated BEM result, which is considered as the best possible reference result.

V. CONCLUSIONS

A new hybrid method (ESIEBEM) combining a technique which is an extension of geometrical-acoustics, the edge source integral equation method (ESIE), and a wave-based technique, the boundary element method (BEM), has been introduced in this paper. A benchmark case has been presented to study the performance of the proposed ESIEBEM method: the study of the scattering by a rigid cube for plane wave incidence; with receivers around the cube, not very close to the cube surface.

The results obtained by the ESIEBEM have been compared with those given by the boundary element method (BEM) and the edge diffraction based method (ESIE). Computations have been carried out with several different discretizations, and linear extrapolation has been employed to estimate more accurate results than the computed ones. The ESIEBEM inherits the property of the ESIE to give accurate results for convex bodies but has the advantage that it overcomes the singularities of the ESIE for certain receiver positions. Resonances in the reciprocal interior problem are not related to the ESIEBEM and CHIEF points are not needed.

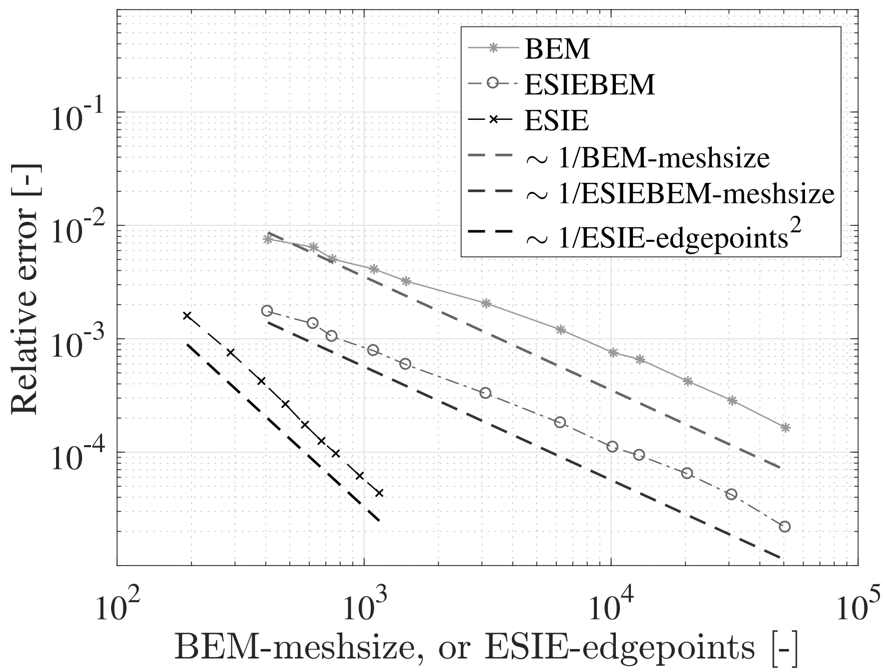

Frequency: 100 Hz

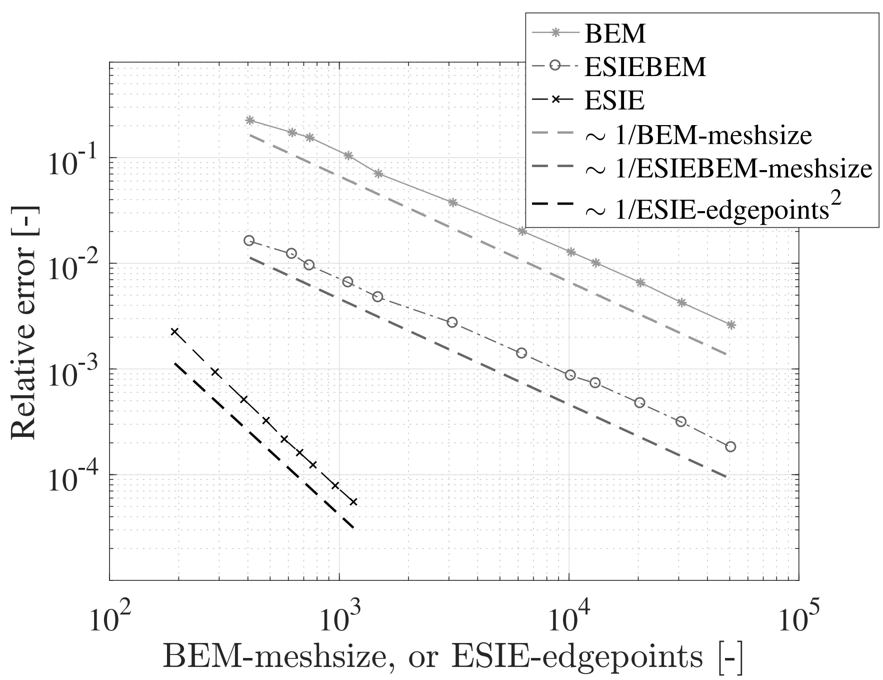

Frequency: 500 Hz

FIG. 7. Median relative error, across all 629 receivers, as a function of number of nodes in the mesh (for the BEM and ESIEBEM) or number of edge integration points (for the ESIE). The reference result is the linear regression extrapolation for each method respectively. Calculated frequencies: a) 100 Hz and b) 500 Hz.

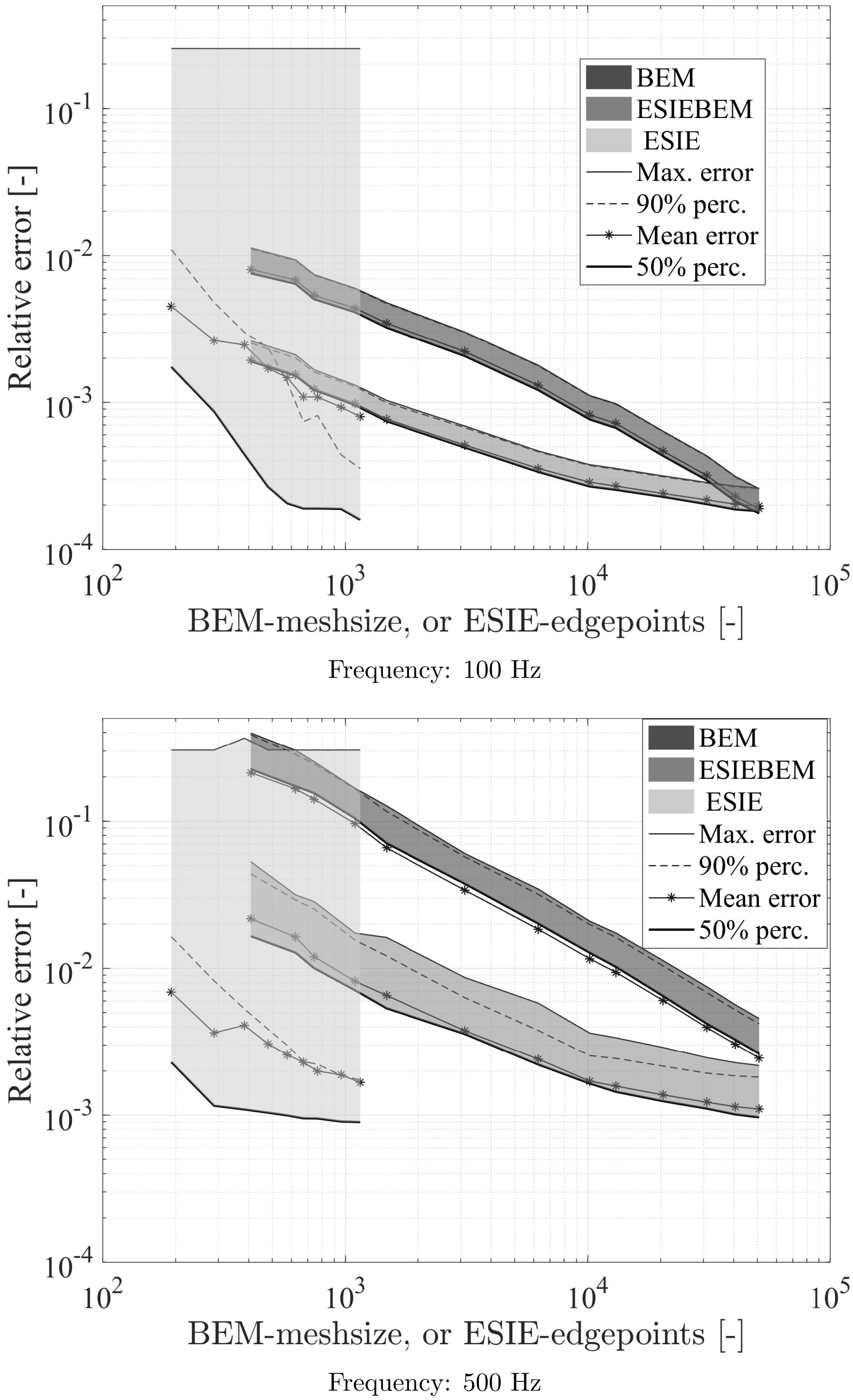

FIG. 8. Relative error, across all 629 receivers, as a function of number of nodes in the mesh (for the BEM and ESIEBEM) or number of edge integration points (for the ESIE). The reference result is the linear regression extrapolation of BEM for all three methods. The frequency is a) 100 Hz and b) 500 Hz.

The computational time for the ESIE and ESIEBEM seems advantageous compared to the BEM for the cube test case. The ESIEBEM also shows good accuracy compared to the BEM and the ESIE. The convergence for two receivers was investigated in detail and the ESIEBEM converges to the similar value as the ESIE. The relative errors of the ESIE and ESIEBEM typically (90% quartile) reach $4 \cdot 10^{-4}$(ESIE) and $3 \cdot 10^{-4}$ (ESIEBEM) at 100 Hz, and $2 \cdot 10^{-3}$ at 500 Hz, relative to the extrapolated BEM result, which is considered as the best possible reference result.

VI. ACKNOWLEDGEMENTS

This paper is part of the project "Hybrid method for calculating the radiated sound from vibrating structures" which has received funding from The Research Council of Norway through a FRIPRO Mobility Grant, contract no 240278/F20. The FRIPRO Mobility grant scheme (FRICON) is co-funded by the European Unions Seventh Framework Programme for research, technological development and demonstration under Marie Curie grant agreement no 608695.

This work was carried out during the tenure of an ERCIM 'Alain Bensoussan' Fellowship Programme.

The authors would like to thank two anonymous reviewers for very helpful suggestions that improved the manuscript.

VII. APPENDIX A: DIRECTIVITY FUNCTION FOR RECEIVERS ON THE SURFACE

The directivity function β in Eq. (3), also used in Eq.(4), is defined by

$$\beta(R, z, S) = \sum_{i=1}^{4} \frac{\sin(\nu\theta_i)}{\cosh(\nu\eta) - \cos(\nu\theta_i)}, \tag{16}$$

where the angles θ_i are

$$\theta_1 = \pi + \theta_S + \theta_R, \qquad \theta_2 = \pi - \theta_S + \theta_R, \tag{17}$$

$$\theta_3 = \pi + \theta_S - \theta_R, \qquad \theta_4 = \pi - \theta_S - \theta_R, \tag{18}$$

and η is an auxiliary function defined by

$$\eta = \cosh^{-1}\left(\frac{\cos\varphi_S \cos\varphi_R + 1}{\sin\varphi_S \sin\varphi_R}\right). \tag{19}$$

When the receiver R is placed on the surface, so $\theta_R = 0$, then $\theta_1 = \theta_3$ and $\theta_2 = \theta_4$. Therefore, Eq. (16) is simplified to

$$\beta(R, z, S) = 2 \cdot \left(\frac{\sin(\nu\pi + \nu\theta_S)}{\cosh(\nu\eta) - \cos(\nu\pi + \nu\theta_S)} + \frac{\sin(\nu\pi - \nu\theta_S)}{\cosh(\nu\eta) - \cos(\nu\pi - \nu\theta_S)}\right), \tag{20}$$

By using the trigonometric identities

$$\sin(\nu\pi - \nu\theta_S) = \sin(\nu\pi)\cos(\nu\theta_S) - \cos(\nu\pi)\sin(\nu\theta_S), \qquad \sin(\nu\pi + \nu\theta_S) = \sin(\nu\pi)\cos(\nu\theta_S) + \cos(\nu\pi)\sin(\nu\theta_S), \tag{21}$$

$$\cos(\nu\pi - \nu\theta_S) = \cos(\nu\pi)\cos(\nu\theta_S) + \sin(\nu\pi)\sin(\nu\theta_S), \qquad \cos(\nu\pi + \nu\theta_S) = \cos(\nu\pi)\cos(\nu\theta_S) - \sin(\nu\pi)\sin(\nu\theta_S), \tag{22}$$

and the equality

$$\sin(\nu\pi)\cos(\nu\pi) = \frac{\sin(2\nu\pi)}{2}, \tag{23}$$

Eq. (20) can be rewritten as

$$\beta(R, z, S) \; = 4 \cdot \left(\frac{\sin(\nu\pi)\cos(\nu\theta_S)\cosh(\nu\eta) - \dfrac{\sin(2\nu\pi)}{2}}{(\cosh^2(\nu\eta) - 2\cosh(\nu\eta)\cos(\nu\pi)\cos(\nu\theta_S) + \cos(\nu(\pi - \theta_S))\cos(\nu(\pi + \theta_S))} \right). \tag{24}$$

This expression is used in the ESIEBEM to compute the first order diffraction component in Eq. (3) at the collocation points on the scatterer's surface. Interestingly enough, the directivity function $\beta(R, z_1, z_2)$ used to obtain the higher order diffraction term in Eq. (6) can also be reduced from Eq. (24). Since z_2 is on the surface, $\theta_S = \theta_{z_2} = 0$ and the simplified expression for $\beta(R, z_1, z_2)$ turns to be

$$\beta(R, z_1, z_2) = 4 \cdot \left(\frac{\sin(\nu\pi)\cosh(\nu\eta) - \dfrac{\sin(2\nu\pi)}{2}}{(\cosh(\nu\eta) - \cos(\nu\pi))^2} \right), \tag{25}$$

where η is defined in Eq. (19).

VIII. APPENDIX B: THE SPARSENESS OF THE H-MATRIX FOR THE ESIE

The sparsity of the **H**-matrix in Eq. (11) can be understood as follows. For simplicity a cube is chosen as scattering object such that all the edges have the same length. The number of discretization points per edge is denoted with $N_{\text{per edge}}$. Each edge point can then see $6N_{\text{per edge}}$ other edge points, because each edge can see exactly 6 of the 12 edges of the cube. Other polyhedral shapes than the cube will have other values than 6/12. There are altogether 12 edges and consequently a total of $N_{\text{total}} = 12N_{\text{per edge}}$ edge discretization points. The number of unknowns (edge source amplitudes $q(z_1, z_2)$) is then $N_{\text{unknowns}} = 12N_{\text{per edge}} \cdot 6N_{\text{per edge}} = 0.5N_{\text{total}}^2$. Thus, the vector $\mathbf{q}$ and the transfer matrix $\mathbf{H}$ will have sizes of $[0.5N_{\text{total}}^2, 1]$ and $[0.5N_{\text{total}}^2, 0.5N_{\text{total}}^2]$ respectively. Each row in this **H**-matrix will obviously have $0.5N_{\text{total}}^2$ elements, but since each edge source can be reached only by $0.5N_{\text{total}}$ other edge sources, only $0.5N_{\text{total}}$ entries in each row will be non-zero. Altogether, the **H**-matrix has $0.25N_{\text{total}}^3$ non-zero elements of all its $0.25N_{\text{total}}^4$, which represents a high degree of sparseness.

The computational cost for obtaining the edge source amplitudes $\mathbf{q}_{\text{final}}$ is given by setting up the **H**-matrix and the iterative solution of Eq. (11), so the calculation time, T, will be

$$T_{\mathbf{q}_{\text{final}}} = C_{\text{set-up}} N_{total}^3 + C_{\text{iter.}} N_{\text{truncation}} N_{total}^3 \sim (1 + C_{\text{iter.,rel.}} N_{\text{truncation}}) N_{total}^3 \quad (26)$$

where the various C are constants, and the value of $N_{\text{truncation}}$ is typically below 20[23].

Finally, the higher-order diffraction sound pressure at $N_{\text{receivers}}$ receiver points is obtained by calculating the double integral in Eq. (6), which is computed for the same discretization as described above. The time for this stage will be

$$T_{\text{prop.}} \sim N_{\text{receivers}} N_{\text{unknowns}} \sim N_{\text{receivers}} N_{\text{total}}^2. \tag{27}$$

As indicated by Eqs. (26) and (27), the calculation of the $\mathbf{q}_{final}$ is typically the dominating computational stage, but for the application here, the number of receiver points is high, so the propagation stage might be significant.

REFERENCES

[1] R. Coifman, V. Rokhlin, and S. Wandzura, "The fast multipole method for the wave equation: A pedestrian prescription," IEEE Antennas and Propagation Magazine **35**(3), 7 – 12 (1993) doi: http://dx.doi.org/10.1109/74.250128.

[2] A. Asheim and U. P. Svensson, "An integral equation formulation for the diffraction from convex plates and polyhedra," The Journal of the Acoustical Society of America **133**(6), 3681–3691 (2013) doi: http://dx.doi.org/10.1121/1.4802654.

[3] U. P. Svensson, H. Brick, and J. Forssén, "Benchmark cases in 3d diffraction with different methods," in *Proceedings of the 7th Forum Acusticum*, Krakow, Poland (2014).

[4] S. R. Martin, U. P. Svensson, J. Slechta and J. O. Smith, "A hybrid method combining the edge source integral equation and the boundary element method for scattering problems," Proceedings of Meetings on Acoustics **26**(1), 015001 (2016), doi: 10.1121/2.0000226.

[5] A. J. Burton and G. F. Miller, “The application of integral equation methods to the numerical solution of some exterior boundary-value problems,” Proceedings of the Royal Society of London A: Mathematical, Physical and Engineering Sciences **323**(1553), 201–210 (1971) doi: 10.1098/rspa.1971.0097.

[6] H. A. Schenck, “Improved integral formulation for acoustic radiation problems,” The Journal of the Acoustical Society of America **44**(1), 41–58 (1968) doi: http://dx.doi.org/10.1121/1.1911085.

[7] J. B. Keller, “Geometrical theory of diffraction,” Journal of the Optical Society of America **52**(2), 116–130 (1962).

[8] R. G. Kouyoumjian and P. H. Pathak, “A uniform geometrical theory of diffraction for an edge in a perfectly conducting surface,” Proceedings of the IEEE **62**(11), 1448–1461 (1974).

[9] R. Ciskowski and C. Brebbia (Eds.), *Boundary Element Methods in Acoustics*, Computational engineering (Netherlands, 1991) (1991).

[10] S. Marburg and S. AMINI “Cats eye radiation with boundary elements: Comparative study on treatment,” Journal of Computational Acoustics **13**(01), 21-45 (2005).

[11] G. Krishnasamy, F. J. Rizzo, and Y. Lie, “Boundary integral equations for thin bodies,” International Journal for Numerical Methods in Engineering **37**, 107–121 (1994).

[12] V. Cutanda Henriquez, P. M. Juhl, and F. Jacobsen, “On the modeling of narrow gaps using the standard boundary element method,” The Journal of the Acoustical Society of America **109**(4), 1296–1303 (2001) doi: http://dx.doi.org/10.1121/1.1350399.

[13] Y. Liu and F. J. Rizzo, "Scattering of elastic waves from thin shapes in three dimensions using the composite boundary integral equation formulation," The Journal of the Acoustical Society of America **102**, 926–932 (1997).

[14] T. Terai, "On calculation of sound fields around three dimensional objects by integral equation methods," Journal of Sound and Vibration **69**, 71–100 (1980).

[15] U. P. Svensson, P. T. Calamia, and S. Nakanishi, "Frequency-domain edge diffraction for finite and infinite edges," Acta Acustica united with Acustica **95**, 568–572 (2009).

[16] J. J. Bowman, T. B. Senior, and P. L. Uslenghi, *Electromagnetic and acoustic scattering by simple shapes (Revised edition)*, Vol. 1 (Hemisphere Publishing Corp., New York, 1987).

[17] A. Asheim and U. P. Svensson, "Efficient evaluation of edge diffraction integrals using the numerical method of steepest descent," Journal of Acoustical Society of America **128**(4), 1590–1597 (2010).

[18] V. Cutanda Henriquez and P. M. Juhl, "Openbem "open source matlab codes for the boundary element method" [computer program]," (2015) http://www.openbem.dk/.

[19] P. M. Juhl, "The boundary element method for sound field calculations," Ph.D. thesis, Technical University of Denmark, The Acoustics Laboratory, Lyngby, 1993.

[20] V. Cutanda Henriquez and P. M. Juhl, "Openbem - an open source boundary element method software in acoustics.," in *39th International Congress on Noise Control Engineering 2010 (INTER-NOISE 2010)*, Lisbon (2010), pp. 5796–5805.

[21] U. P. Svensson, "Edge diffraction toolbox for matlab [computer program]," http://www.iet.ntnu.no/~svensson/software/index.html.

[22]C. Geuzaine and J.-F. Remacle, "Gmsh: A 3-d finite element mesh generator with built-in pre- and post-processing facilities," International Journal for Numerical Methods in Engineering **79**(11), 1309–1331 (2009) doi: 10.1002/nme.2579.

[23]U. P. Svensson and A. Asheim, "Edge-diffraction based integral equation for the scattering from convex rigid polyhedra," in *Proceedings of the 6th Forum Acusticum*, Aalborg (2011).